ELSEVIER

Thermochimica Acta 371 (2001) 111–119

thermochimica acta

www.elsevier.com/locate/tca

Thermal and geochemical investigation of Seyitomer oil shale

Mustafa Versan Kok[a,*], Ilker Senguler[b], Heinz Hufnagel[c], Nurettin Sonel[d]

[a]*Department of Petroleum and Natural Gas Engineering, Middle East Technical University, 6531 Ankara, Turkey*
[b]*General Directorate of Mineral Research and Exploration of Turkey, 6520 Ankara, Turkey*
[c]*Bundesanstalt fur Geowissenschaften und Rohstoffe, Hanover, Germany*
[d]*Department of Geological Engineering, Ankara University, Ankara, Turkey*

Received 12 September 2000; accepted 12 December 2000

Abstract

The results of an experimental study on the thermal and organic geochemical investigation of Seyitomer oil shale sample are presented. Thermogravimetry (TG/DTG) and differential scanning calorimetry (DSC) have been used to determine the thermal behaviour of the oil shale sample. On the other hand, organic carbon content, rock-eval pyrolysis, and gas and liquid chromatography experiments were conducted to determine geochemical properties of the oil shale sample. © 2001 Elsevier Science B.V. All rights reserved.

Keywords: Oil shale; Thermal analysis; Organic matter; Geochemical analysis

1. Introduction

Oil shale deposits in Turkey are widely distributed in middle and western Anatolian. The information on the deposits is based on borehole data and the oil shales are of Palaeocene–Eocene and middle–upper Miocene age. Current reserves of oil shales in Turkey are ~1865 Mt, located in Seyitomer, Himmetoğlu, Hatıldağ and Beypazarı oil shale fields [1]. The host rocks are marl and clays, in which the organic matter is heterogeneously and finely dispersed. The unstable conditions, which prevailed during the formation and the filling of the basin in the older Neogene, the morphological differentiation of the basin floor by island-like elevations, lateral facies changes, tectonic movements and partial erosion have affected the sediments. Bituminous marl unit crops out around the oil shale field and has been penetrated by many drill holes for lignite prospecting. The unit occurs between the main seam; it consists of a variety of predominantly grey, green–grey and brown marl with intercalated brightly coloured marly limestone, and silicified limestone and chert. The main mineral components of Seyitomer oil shale are quartz, dolomite, muscovite, illite and smectite [2]. The following may occur as trace amounts: feldspars, calcite, pyrophyllite, hornblende, chlorite and aragonite (Table 1). EGOS varies considerably in thickness and quality in the lateral and vertical directions; the thickness ranges from 3 to 29.5 m, the upper calorific value from 3140 to 4250 kJ kg^{-1} and the oil content from 4 to 5.9 wt.% (Table 2).

Thakur and Nuttall [3] studied the pyrolysis kinetics of the thermal decomposition of oil shale by isothermal and non-isothermal thermogravimetry. Their results showed that the thermal decomposition of oil shale involves two consecutive reactions with bitumen as an intermediate. Both reactions follow

* Corresponding author. Tel.: +90-312-210-4891; fax: +90-312-210-1271.
E-mail address: kok@metu.edu.tr (M.V. Kok).

PII: S0040-6031(01)00415-4

Table 1
Mineral composition of oil shale deposits in Turkey[a]

Deposit	Q	Op	F	H	Sm	Mi	K	Ch	Cc	Do	Ar	Ma	Cl	Er	An	He	Ph	Py
Seyitomer	CD	–	SD	T	CD	CD	–	A	SD	CD	A	–	–	–	–	–	–	A

[a] Q: quartz; Op: opal-CT; F: feldspar; H: hornblende; Sm: smectite; Mi: mica-illite; K: potassium; Ch: chlorite; Cc: calcite; Do: dolomite; Ar: aragonite; Ma: magnesite; Cl: Clinoptilolite; Er: erionite; An: analcite; He: heulandite; Ph: phillipsite; Py: pyrite; CD: co-dominant; SD: sub-dominant; A: accessory; T: trace.

first-order kinetics. Among three models used Antony–Howard model yields lower deviation and thus provides a better fit of the data. Skala and Sokic [4] developed a kinetic expression commonly used in the thermal analysis of oil shale pyrolysis which was derived on the basis of a simple first-order kinetic equation of kerogen decomposition. There was an increase in the activation energy with increasing content of paraffinic structures in the oil shale. Rejeshwar [5] studied the pyrolysis kinetics of thermal decomposition of Green River oil shale kerogene by non-isothermal thermogravimetry. He critically reviewed the factors influencing kinetic data such as sample order geometry, heating rate and atmosphere. Shih and Sohn [6] used non-isothermal thermogravimetry with a variety of heating rates to the determination of kinetic parameters for Green River oil shale pyrolysis. Four different methods were employed for kinetic analysis and the results appear to be in fair agreement. Lee et al. [7] studied the thermal behaviour of oil shale as a function of grade, gas composition and particle size. Two exothermic peaks are generated by oil shale heated in air. The first peak can be assigned to the combustion of light hydrocarbon fractions from the shale organic matter whereas the second peak arises from the oxidation of char. Skala et al. [8] investigated the pyrolysis kinetics of oil shales under non-isothermal conditions using thermal methods. The results obtained were incorporated into the multi-step kinetic model which was adjusted according to the specific purposes of particular oil shale samples and tested by comparison of the experimental and simulated thermogravimetry (TG/DTG) and differential scanning calorimetry (DSC) curves. Levy and Stuart [9] obtained TG/DTG curves of Australian oil shales and kerogen concentrates heated in a dynamic air atmosphere. It was observed that the combustion of kerogen occurs in two stages, indicated by two sharply defined peaks. Kok et al. [10–13] determined the thermal characteristics and kinetic parameters of oil shales by thermal analysis methods both for pyrolysis and combustion. Kinetic parameters of the samples are determined with different kinetic models and the effect of pressure was also determined. Brukner-Wein et al. [14] studied the organic matter of Pliocene oil shales from maar-type twin creaters by different analytical techniques as rock-eval pyrolysis, bitumen analysis, FTIR, elemental analysis and pyrolysis of the insoluble material. It was found that the organic-rich, alginitic layers were deposited at the same time, under the same palaeo-climatic conditions and have basically similar lithologies. Seewald et al. [15] studied experimentally the organic–inorganic interactions during vitrinite maturation of organic-lean middle valley sediment. Inorganic fluid composition was monitored as a function of time, and vitrinite reflectance was measured at the termination of each experiment. Results of this study demonstrate that the geochemical environment surrounding vitrinite influences the rate of maturation. Borrego et al. [16] studied the aliphatic fraction of the bitumens from three bands of the oil shale by gas chromatography and

Table 2
Characteristics of Seyitomer oil shale

Deposit	Calorific value (MJ kg^{-1})	Total organic carbon (wt.%)	Oil content (wt.%)	Total sulphur (wt.%)	Reserves (Mt)
Seyitomer	3.55	6.9	5	0.9	110

gas chromatography/mass spectrometry. The biomarker maturity ratios indicate that the oil shales have similar maturities and are close to the onset of oil generation.

The aim of this research is to identify the thermal behaviour and kinetics of Seyitomer oil shale sample and characterisation of the organic matter with respect to maturity and type of the organic matter.

2. Experimental

Initially, thermal experiments were performed with a Du Pont 951 TG/DTG and 910 DSC equipments. DSC monitored the differential heat flow of the samples whereas TG/DTG measured the mass loss or rate of loss either as a function of temperature or time in a varied but controlled atmosphere. The experimental procedure involves placing ~10 mg of sample, within the instruments setting the heating rate and flow rate of the purge gas (air) then commencing the experiment. Experiments by both TG/DTG and DSC were performed at 10°C min^{-1} heating rate over the temperature range 20–600°C with an air flow rate of 50 cm^3 min^{-1}. The oil shale sample used had particle sizes <60 mesh and prepared according to ASTM (ASTM D 2013-72) standards. In order to assess the reproducibility, experiments were performed twice.

In the second part, experiments were performed to characterise the organic matter with respect to maturity and type of the organic matter. Organic carbon content of the sample were determined with a LECO CS 444 analyser after removing carbonate with hot 2 N HCl. Rock-eval pyrolysis experiments were performed with a Rock-Eval 5 equipment. S_1 (amount of hydrocarbons volatile at 300°C), S_2 (amount of hydrocarbons volatile at a programmed temperature between 300 and 650°C), and T_{max} (temperature of S_2 (maximum)) values were determined. Hydrogen index (HI) was equal to S_2 normalised to TOC and the generation potential (GP) was determined as the sum of $S_1 + S_2$. Extraction of the soluble organic matter was determined with acetone/hexane (1:1) in a Soxtex device. Precipitation of asphaltenes was carried out with petroleumbenzene/dichloromethane (30:1). Separation of the deasphalted extracted into the saturated hydrocarbons, aromatic hydrocarbons and hetero-compounds was carried out by liquid chromatography on silica gel and aluminium oxide. Analysis of the saturated fraction was carried out with a Hewlett Packard 5890 gas chromatograph connected to a HP 5972 mass selective detector, using 30 m fused silica DB 5 capillary column. For the identification of the normal- and cyclo-alkanes, mass spectra and retention times were used.

3. Results and discussion

Studies on oil shale using thermal analysis techniques have shown that combustion of indigenous organic matter is a complex multi-stage process. The thermal behaviour of oil shale in dynamic air atmospheres may exhibit characteristics of both the inorganic (mineral) and organic (kerogen + bitumen) components. The low temperature portion of the thermal curves may represent thermal decomposition identical to that observed in inert atmospheres, while at higher temperatures oxidative characteristics of the organic component generally predominate. The oxidation process of Seyitomer oil shale showed an exothermic behaviour at around 310°C on DSC curves depending on the heating rate (Fig. 1). The shoulder on the high temperature side of the reaction region was attributed to the possible swelling of the sample, resulting in an impermeable mass that reduced the oxygen accessibility, causing a decrease in the reaction rate. TG/DTG curves of Seyitomer oil shale (Fig. 2) showed the same reactivity region as DSC curves.

Non-isothermal kinetic study of weight loss under pyrolysis and combustion processes is extremely complex for oil shales because of the presence of the numerous complex components and their parallel and consecutive reactions. In this research, Coats and Redfern [17] model based on Arrhenius theory was used for kinetic analysis of the data generated by the TG/DTG experiments.

The calculation of the kinetic data is based on the formal kinetic equation

$$\frac{d\alpha}{dt} = k\alpha^n \quad (1)$$

where α is the amount of sample undergoing the reaction, n the order of reaction and k the specific

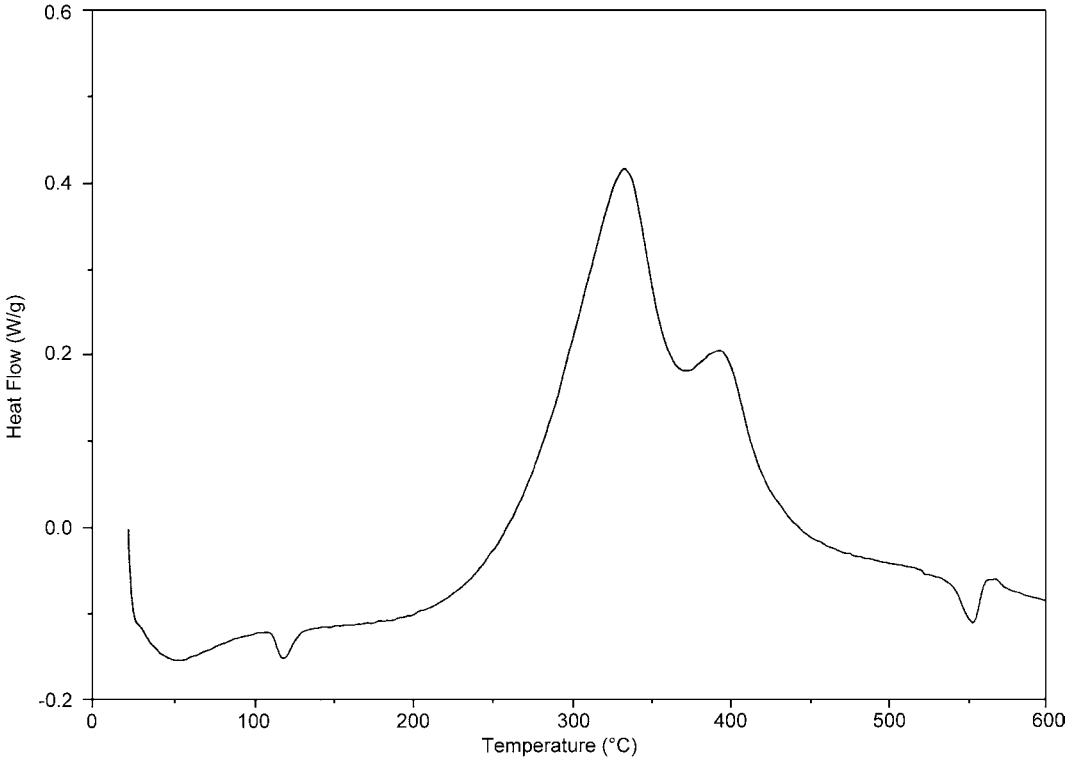

Fig. 1. DSC curve of Seyitomer oil shale (10°C min^{-1}).

rate constant. The temperature dependence of k is expressed by the Arrhenius equation

$$k = A \exp\left(\frac{-E}{RT}\right) \tag{2}$$

where A is the Arrhenius constant, E the activation energy and R the gas law constant.

Coats and Redfern developed an integral method, which can be applied to TG/DTG data, assuming the order of reactions. The correct order is presumed to lead to the best linear plot, from which the activation energy is determined. The form of the equation, which is use for analysis:

$$\ln\left[1 - \frac{(1-\alpha)^{1-n}}{T^2(1-n)}\right] = \ln\left[\left(\frac{AR}{\beta E}\right)\left(1 - \frac{2RT}{E}\right)\right] - \left[\frac{E}{RT}\right] \tag{3}$$

where β is the heating rate.

Thus, a plot of $\ln[1 - (1-\alpha)^{1-n}/T^2(1-n)]$ vs. $1/T$ should result in a straight line of slope equals $-E/R$ for the correct value of reaction order n. In this research, five different reaction orders, $\frac{1}{2}, \frac{2}{3}, 1, \frac{3}{2}$ and 2, were assumed and coefficient of determinations of each reaction were calculated. Highest correlation coefficient was found at a reaction of unity (Table 3).

The results of rock-eval pyrolysis are given in Table 4. From the plot of Langford and Blanc-Valleron [18], a mean hydrogen index of 556 mg C_{pyr}/gC can be calculated for the Seyitomer oil shale (Fig. 3). Taking into account that whole rock samples instead of kerogens were used, a type I/II kerogen can be assumed. T_{max}-values scatter around 430°C which would indicate reflectance of around 0.5%. Because of the amount and composition of the soluble organic matter, this value seems to be too high.

For the analysis of the soluble organic matter, two samples with moderate and a high organic carbon content were selected. The results are given in Table 5. The amount of soluble is fairly high which would qualify the samples as oil source rocks. Because of the low amounts of hydrocarbons in the extracts,

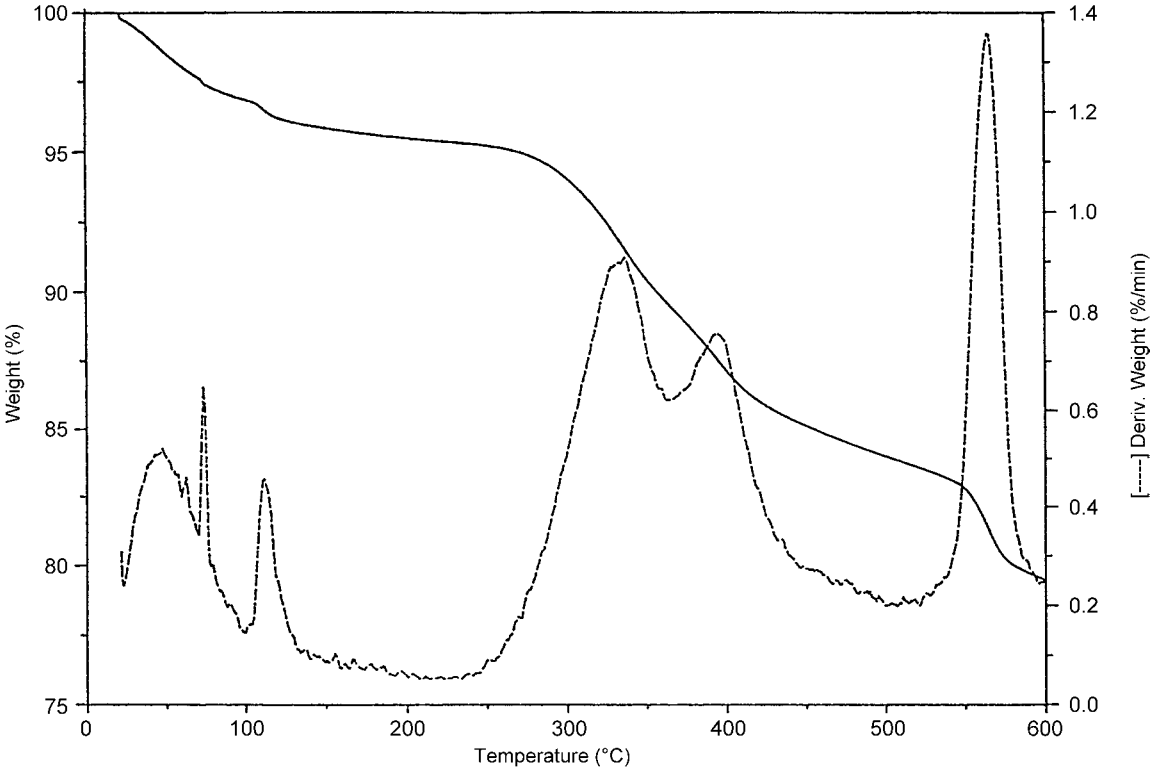

Fig. 2. TG/DTG curve of Seyitomer oil shale (10°C min^{-1}).

Table 3
Peak reaction temperatures and kinetic parameters of Seyitomer oil shale

Sample	Peak reaction temperature (°C)		Activation energy (kJ mol^{-1})	
	DSC	TG/DTG	Region I	Region II
Seyitomer	340	565	73.8	5.9

Table 4
Organic carbon and rock-eval data from Seyitomer oil shales

CO–Nr	K–Nr	Stratigr.	Depth (m)	TOC (%)	S_1 (kg t^{-1})	S_2 (kg t^{-1})	HI (MgC/gC)	GP (kg t^{-1})	PI ($S_1/(S_1+S_2)$)	T_{max} (°C)
42412	14698	Miocene	34	3.71	0.46	16.79	453	17.25	0.03	431
42413	14703	Miocene	39	7.24	0.77	42.17	582	42.94	0.02	434
42414	14708	Miocene	44	13.2	2.53	81.06	614	83.59	0.03	430
42415	14713	Miocene	49	6.52	1.27	38.71	594	39.98	0.03	430
42416	14718	Miocene	54	5.89	0.96	32.32	545	33.28	0.03	428
42417	14723	Miocene	59	13.1	2.09	93.37	713	95.46	0.02	436
42418	14726	Miocene	62	17.9	1.95	86.25	482	88.20	0.02	433

Table 5
Extract content and composition of Seyitomer oil shale[a]

CO–Nr	Depth (m)	TOC (%)	Sol (ppm)	Sol/TOC	Sat		Aro		Het		Asph		Loss (%)	Sat/Aro
					ppm	%	ppm	%	ppm	%	ppm	%		
42413	39	7.24	3600	4.97	121	3.4	257	7.1	1123	31.2	1084	30.1	28.2	0.47
42417	59	13.1	7784	5.94	133	1.7	340	4.4	1534	19.7	4038	51.9	22.3	0.39

[a] TOC: total organic carbon, Sol: soluble organic matter, Sat: saturated hydrocarbons, Aro: aromatic hydrocarbons, Het: heterocompounds, Asph: asphaltenes.

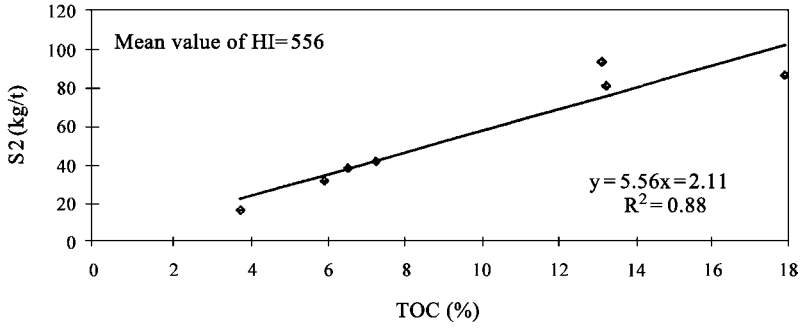

Fig. 3. TOC (%) vs. S_2 (kg t^{-1}) curve of Seyitomer oil shale.

however, the samples plot (Fig. 4) into the ''gas field'', which means, in this case that the shales are too immature to generate liquid hydrocarbons. So, a vitrinite reflectance of 0.5% has certainly not been reached.

Plots of GC–MS analysis are given in Fig. 5. Because of the close similarity in the composition of the saturated fraction of both samples, despite the difference in the overall amount of the organic matter, only the chromatograms of sample CO 42413 are

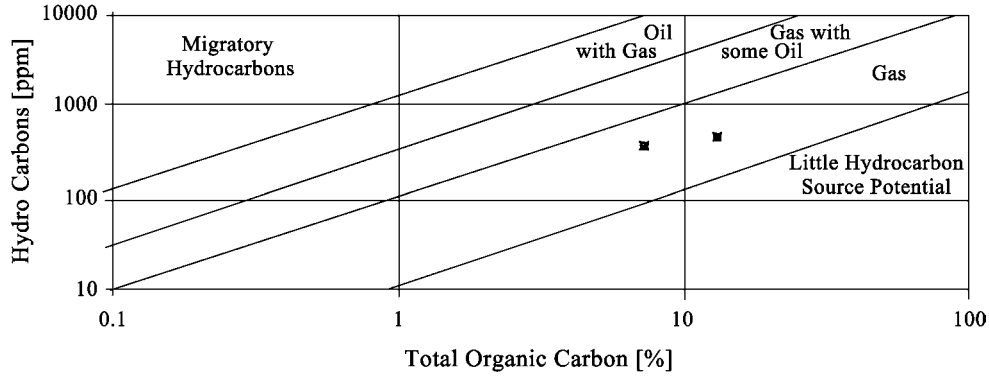

Fig. 4. TOC (%) vs. hydrocarbons (ppm) curve of Seyitomer oil shale.

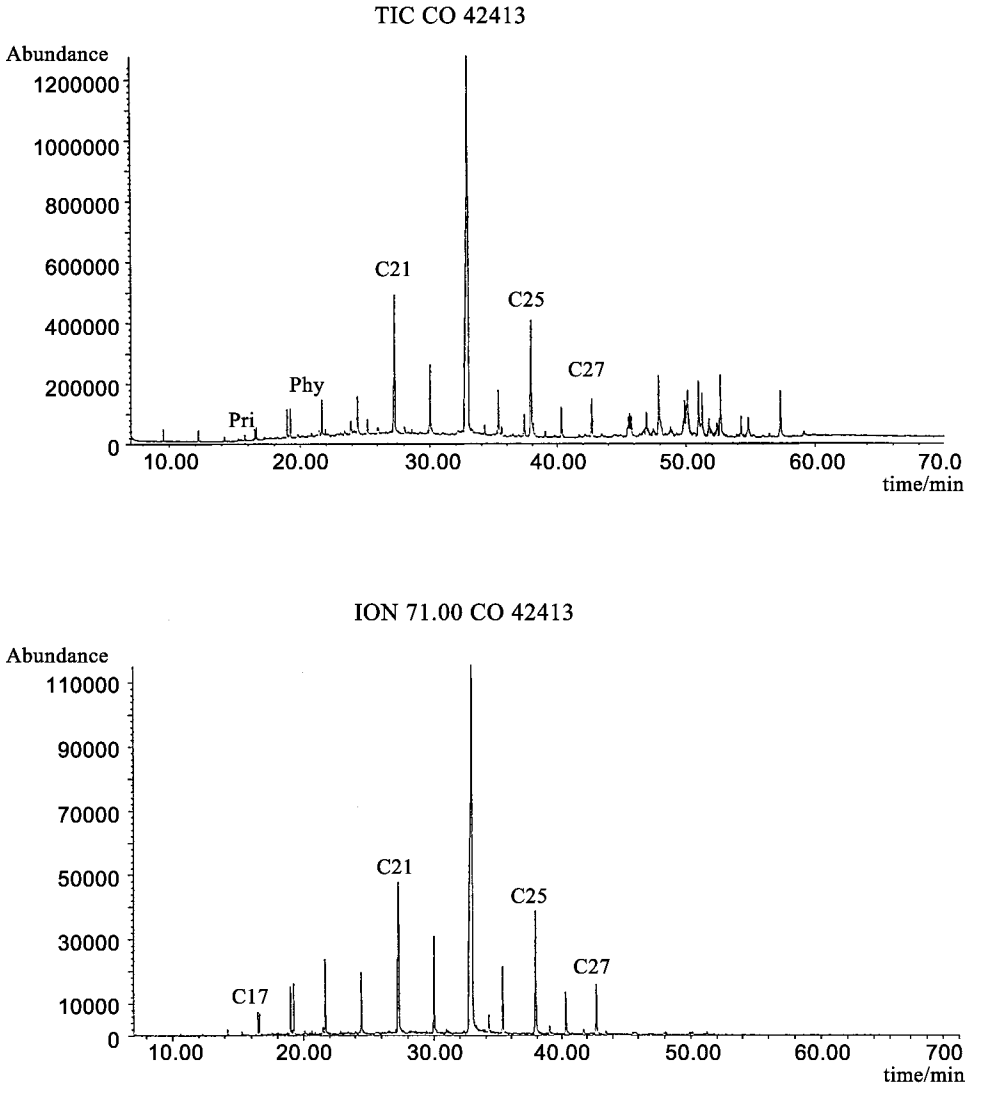

Fig. 5. Total ion content vs. alkanes (*m/z* 71) curve of Seyitomer oil shale.

presented. The TIC trace is dominated by the occurrence of *n*-alkanes having 17–27 carbon atoms. A marked odd–even predominance with C23 as main compound can be observed. The isoprenoids pristane and phytane are fairly high concentrated, the ratio pristane to phytane is below 1. In the high boiling range, a series of compounds could be tentatively identified by means of mass spectra and literature data as triterpenes, strenes and steranes (Fig. 6). The strong prevalence of the odd-numbered *n*-alkanes as well as the occurrence of unsaturated triterpenoids (hopenes and strenes) and hopanoids with 17β-, 21β-configuration are a prove of the immature character of the samples [19]. The sources of the organic matter seem to be algae and bacteria (microbial mats), as odd-numbered long-chain *n*-alkanes (C29, C31) are lacking. The hopanoids can be traced back to microbial origin as well. The low pristane/phytane ratios are indicative of an anoxic or dysoxic sedimentary environment.

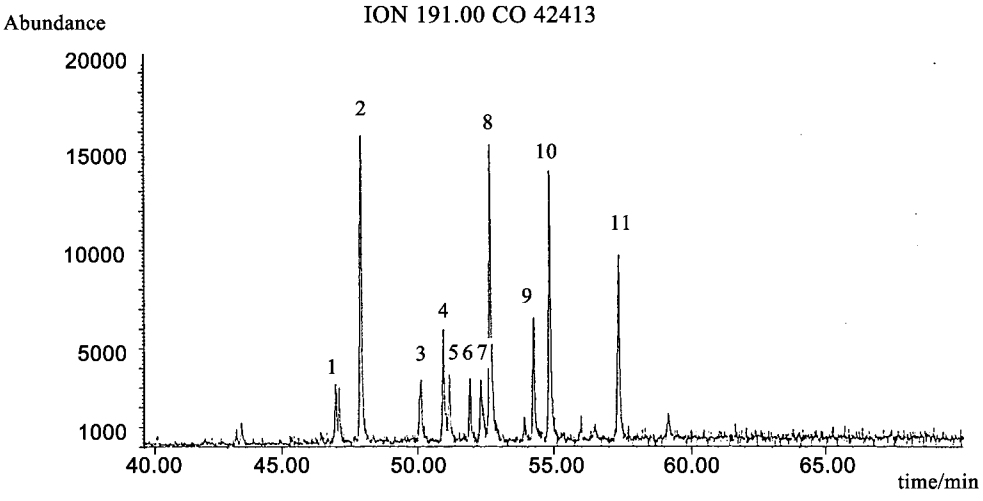

1 = trisnorhop-17(21)-ene, **2** = 17β[H]22,29,30 trisnorhopane, **3** = norhop-17(21)-ene, **4** = hop-17(21)-ene, **5** = normoretane, **6** = hopane, **7** = moretane, **8** = β,β-norhopane, **9** = homohopane, **10** = ββ-hopane, **11** = β,β-homohopane

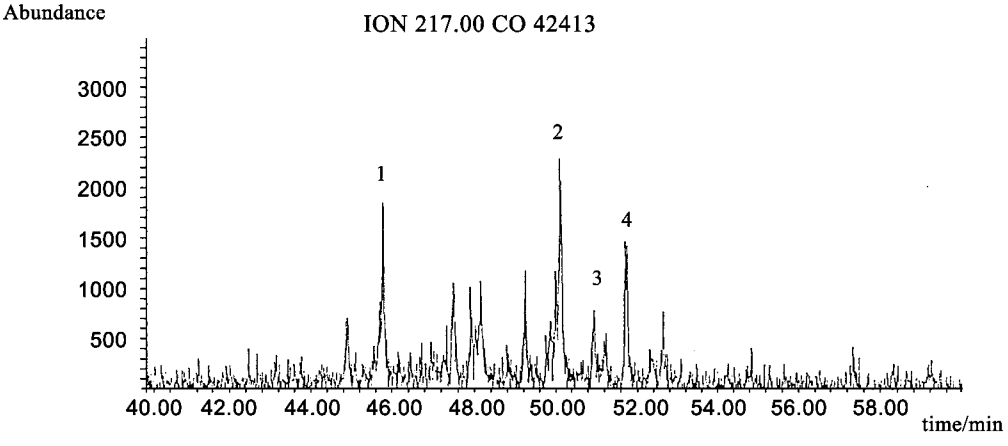

Fig. 6. Triterpanes (*m/z* 191) vs. steranes (*m/z* 217) curve of Seyitomer oil shale.

4. Conclusions

In this research, an experimental study on the thermal and organic geochemical investigation of Seyitomer oil shale sample were presented. The following conclusions were derived from the research conducted:

- The oxidation process of Seyitomer oil shale showed an exothermic behaviour at around 310°C on DSC and TG/DTG curves.
- Taking into account that whole rock samples instead of kerogens were used, a type I/II kerogen can be assumed.

- T_{max}-values scatter around 430°C which would indicate reflectance of around 0.5%.

References

[1] M. Sener, I. Senguler, M.V. Kok, Fuel 74 (1995) 999.
[2] H. Hufnagel, Investigation of oil shale deposits in western Turkey, Technical Report Part 1, Project No. 84.2127.3, Bundesanstalt fur Geowissenschaften und Rohstoffe, Hanover, Germany, 1989.
[3] D.S. Thakur, H.E. Nuttall, Ind. Eng. Chem. Res. 26 (1987) 1351.
[4] D. Skala, M. Sokic, J. Therm. Anal. 37 (1992) 729.
[5] K. Rajeshwar, Thermochim. Acta 45 (1992) 253.
[6] S.M. Shih, H.Y. Sohn, Ind. Eng. Chem. Process. Des. Dev. 19 (1980) 420.
[7] I.C. Lee, M.D. Lee, H.Y. Dohn, Thermochim. Acta 84 (1985) 371.
[8] D. Skala, H. Kopsch, M. Sokik, H.I. Neum, A. Boucnovic, Fuel 65 (1990) 490.
[9] J.H. Levy, W.I. Stuart, Thermochim. Acta 74 (1984) 227.
[10] M.V. Kok, R. Pamir, J. Therm. Anal. Calorimetry 53 (1998) 567.
[11] M.V. Kok, J. Sztatisz, G. Pokol, J. Therm. Anal. Calorimetry 55 (1999) 939.
[12] M.V. Kok, R. Pamir, J. Therm. Anal. Calorimetry 56 (1999) 953.
[13] M.V. Kok, R. Pamir, J. Anal. Appl. Pyrolysis 55 (2000) 185.
[14] A. Brukner-Wein, C. Sajgo, M. Hetenyi, Org. Geochem. 31 (2000) 453.
[15] J.S. Seewald, L.B. Eglington, Y.L. Ong, Geochim. Cosmochim. Acta 64 (2000) 1577.
[16] A.G. Borrego, P. Bernard, C.G. Blanco, Appl. Geochem. 14 (1999) 1049.
[17] A. Coats, J. Redfern, Nature 201 (1964) 68.
[18] F.F. Langford, M. Blanc-Valleron, American Association of Petroleum Geologist 74 (6) (1990) 799.
[19] K.E. Peters, J.M. Moldowan, The Biomarker Guide. Interpreting Molecular Fossils in Petroleum and Ancient Sediments, Prentice-Hall, Englewood Cliffs, NJ, 1993.